Available online at www.sciencedirect.com
SCIENCE DIRECT®
Journal of Biotechnology 105 (2003) 11–31
JOURNAL OF Biotechnology
www.elsevier.com/locate/jbiotec

Gene expression patterns for metabolic pathway in *pgi* knockout *Escherichia coli* with and without *phb* genes based on RT-PCR

Md. Mohiuddin Kabir [a], Kazuyuki Shimizu [a,b,*]

[a] *Department of Biochemical Engineering and Science, Kyushu Institute of Technology, Iizuka, Fukuoka 820-8502, Japan*
[b] *Institute for Advanced Biosciences, Keio University, Tsuruoka, Yamagata 997-0017, Japan*

Received 4 December 2002; received in revised form 1 May 2003; accepted 26 May 2003

Abstract

Metabolic regulations were investigated from the viewpoint of gene expressions for *Escherichia coli* JM109 and *pgi* knockout *E. coli* with and without *phb* genes using RT-PCR. One of the main features of *pgi* knockout *E. coli* is the overproduction of NADPH produced in pentose phosphate (PP) pathway. NADPH overproduction in PP pathway in *pgi* mutant causes some reducing power imbalance that ultimately affects the cell growth. It was shown that this reducing power imbalance can be recovered to some extent by introducing NADPH absorbing pathway such as PHB synthetic pathway into *pgi* mutant *E. coli*. To get insight into the regulation mechanism of *pgi* mutant *E. coli* at the transcriptional level, 87 *E. coli* genes involved in central metabolic pathways and key regulatory mechanisms were investigated by semi-quantitative RT-PCR analysis. The analysis showed that pentose phosphate pathway genes and part of the glycolysis pathway genes were affected significantly by expression of *phb* genes in *pgi* mutant *E. coli* DF11/pAeKG1 as well as in *pgi* mutant *E. coli* DF11 as compared with those in *E. coli* JM109. In contrast, most of the TCA cycle genes except *icd*A were downregulated in both *pgi* mutants *E. coli*. The upregulation of *icd*A gene may be due to the positive regulation of *fru*R. Moreover, it was found that *ack* gene as well as *ace*A and *ace*B genes involved in the glyoxylate shunt were upregulated in *pgi* mutants while *ppc* gene was downregulated, indicating that *pgi* inactivation changes the anaplerotic pathway from *ppc* pathway to glyoxylate shunt. Enzyme activities of *glk*, *zwf*, *tpi*A, *fba*A, *ldh*A, *glt*A, *ace*A, *mdh* and *mae*B were also measured and compared with the corresponding gene expressions. Most of them are well correlated except for *ace*A gene indicating that glyoxylate pathway is regulated on the protein level, not on the gene level.

Keywords: RT-PCR; *pgi* mutant *E. coli*; *phb* genes; NADPH; *ace*A

1. Introduction

It is becoming more and more important to analyze the cell in vivo. For this, it is important to analyze the cell as a whole or as a system. The

* Corresponding author. Tel.: +81-948-29-7817; fax: +81-948-29-7801.
E-mail address: shimi@bse.kyutech.ac.jp (K. Shimizu).

0168-1656/03/$ - see front matter © 2003 Elsevier B.V. All rights reserved.
doi:10.1016/S0168-1656(03)00170-6

present research is, therefore, focused on the global metabolic regulation analysis based on the gene expression patterns. Expression profiling is a powerful tool for analyzing gene expression at a genomic scale. It can be used to compare global changes in gene expression that occur in response to environmental stimulus or to compare the effects of genetic changes on gene expression. This analysis can provide important information about cell physiology and has the potential to identify connections between regulatory or metabolic pathways that were not previously known. The use of gene arrays to analyze gene expression has been used extensively for eukaryotic systems (DeRisi et al., 1997; Iyer et al., 1999). Recently, its usefulness for analyzing gene expression has also been demonstrated for prokaryotes (Arfin et al., 2000; Richmond et al., 1999; Tao et al., 1999; Wilson et al., 1999). Since biotechnological research and its application require the knowledge on how genes work at the genomic scale, DNA microarray has been extensively used in the past several years for this purpose to reveal global regulation. As illustrated in *S. cerevisiae*, cell metabolism adapts to the environment during growth in a chemostat culture (Ferea et al., 1999). The transcript levels of approximately 10% of the genes were changed more than twofold after 250 generations in the fermentor. This kind of investigation is useful in analyzing the physiological changes and detecting the effects of gene structure changes for strain improvement (Kao, 1999).

In this study, we investigated how gene expression patterns change for *pgi* knockout *E. coli* with or without *phb* genes as compared with that of *E. coli* JM109 using RT-PCR. In RT-PCR, an RNA template is copied into a complementary DNA transcript (a cDNA) using a retroviral reverse transcriptase. The cDNA is then amplified exponentially using PCR. This product can be used to detect or quantify the expression (Dieffenbach and Dveksler, 1995; Siebert and Larrick, 1991). RT-PCR has been applied to detect changes in absolute and relative amounts of specific RNAs (Arcelana-Panlilio and Schultz, 1993). The latter is also called semi-quantitative RT-PCR. RT-PCR is more sensitive and easier to perform as compared with other RNA analysis techniques, including Northern blots, RNase protection assays, in situ hybridization, and S1 nuclease assays (Foley et al., 1993; Mocharla et al., 1990). Comparing with Northern analysis, which has been used routinely to visualize specific mRNA levels, RT-PCR offers several advantages such as (1) much less amount of total RNA is required; (2) the low abundance transcripts of interest, which cannot be detected by Northern blotting, can be quantified reproducibly by RT-PCR; (3) the variable expression of multiple mRNAs can in principle be analyzed simultaneously by RT-PCR, which is difficult to realize by the traditional methods; (4) the RT-PCR procedure requires only a few hours to perform. Generally, two types of RT-PCR approaches have been used until now. The most popular method involves the use of an internal standard to control variations in PCR amplification efficiency and to determine the amount of transcript in original samples (Singer-Sam and Riggs, 1993). Although this method can be used to detect small changes in mRNA levels, it requires not only the additional steps to prepare the internal standard, but also necessitates performing several PCR reactions to quantify each sample of mRNA. Therefore, this method is time-consuming, complicated and not useful for rapid quantification of multiple samples. Another approach (Harrison et al., 2000; Kwon et al., 2000) relies on adjustment of the amount of input RNA and the number of cycles of PCR to assure that measurement is done in the exponential phase of PCR when the signal is proportional to the amount of input template or the number of cycles. This method is reproducible for measurement of relative changes in mRNA levels if the following two conditions are met. First, tube to tube variation must be minimal so that a constant value can be assumed in all related PCR reactions. Second, all data must be obtained before the reactions begin to reach the plateau phase. Although this method requires a standard curve to determine the level of signal that corresponds to the specific amount of mRNA, it is rapid and simple to quantify the variable expression of mRNAs with sufficient resolution (Akiyama et al., 1996; Brucato et al., 2000).

In this paper, a semi-quantitative RT-PCR was used to investigate the differences in gene expression profiles of a recombinant *Escherichia coli* lacking phosphoglucose isomerase (*pgi*). The *pgi* inactivation in *E. coli* forces glucose catabolism via the pentose phosphate (PP) pathway. As a consequence, metabolic redirection in a *pgi* mutant overproduces NADPH, and thus may inhibit the cell growth due to NADPH imbalance. An interesting idea of incorporating NADPH consuming pathway such as poly(3-hydroxybutyrate) (PHB) synthetic pathway may then arise. For PHB synthesis, three enzymes are necessary from acetyl-CoA such as β-ketothiolase, acetoacetyl-CoA reductase and PHB synthase. Among them, the reaction catalyzed by acetoacetyl-CoA reductase requires NADPH (Kidwell et al., 1995; Lee and Chang, 1995; Shi et al., 1999). Thus, NADPH imbalance in *pgi* mutant may possibly be overcome by incorporating *phb* genes in *E. coli*. In the present research, we analyzed 87 *E. coli* gene expressions in glycolysis, PP pathway, and the tricarboxylic acid (TCA) cycle, etc. by RT-PCR. Moreover, we measured some of the enzyme activities to see the metabolic regulation mechanism from the viewpoint of gene and protein expressions.

2. Materials and methods

2.1. Bacterial strain, plasmid, and growth condition

The strain used in the present study was *E. coli* DF11 (*rps*L176 [*str*R] *met*A28 *pgi*-2 *his*-84) and *E. coli* DF11/pAeKG1 having plasmid that contains the *Ralstonia eutropha* PHB biosynthesis genes (Shi et al., 1999). The PHB biosynthesis genes are constitutively expressed in *E. coli*. As a control, *E. coli* JM109 (*rec*A1 *sup*E44 *hsd*R17 *end*A1 *gyr*A96 *thi rel*A1 Δ[*lac pro*AB] *ka*) was also cultivated. Luria-Bertani (LB) medium containing 20 g l^{-1} glucose as the sole carbon source was used for cell growth. The inoculum was prepared by transferring cells from a glycerol stock (0.1 ml) to a 50-ml L-shaped test tube containing 10 ml of LB medium. The culture was incubated overnight and 1 ml of the broth was then transferred into a 500-ml T-shaped flask containing 100 ml of the LB medium. Ampicillin (50 μg ml^{-1}) was added to maintain the plasmid. The batch cultivation was carried out in a 2-l jar bioreactor (M-100, Rikakikai Co. Ltd., Tokyo, Japan) containing 1 l of LB medium sterilized for 20 min at 121 °C.

2.2. Analytical procedures

Cell concentration was determined by measuring the optical density (OD) of the culture broth with a spectrophotometer (Ubet-30, Jasco Co., Tokyo, Japan) at 600 nm. The OD value was then converted to g DCW l^{-1} (dry cell weight per liter) using the relationship between OD values and DCW obtained previously. The amount of PHB was measured by gas chromatography (GC-8APF/C-R6A, Shimadzu Co., Kyoto, Japan) as described by Braunegg et al. (1978). The acetic acid and lactic acid concentrations were measured by enzymatic kit (Wako Co., Osaka, Japan). Glucose was also measured using an enzymatic kit (Wako Co., Osaka, Japan). The intracellular NADPH concentration was measured according to Bergmeyer (1989).

2.3. Assays for protein and enzyme activity

The Folin and Ciocalteu's phenol reagent was used for the determination of protein concentration, where the method was similar to that described by Lowery et al. (1951). A standard curve was constructed for each experiment using crystalline bovine serum albumin (Sigma Chemical Co., USA). For enzyme assay, aliquots were removed at indicated time intervals, centrifuged and frozen at −20 °C. The samples were thawed on ice, washed with 0.1 M Tris–HCl (pH 7.5) buffer, and resuspended in a 10% volume of the same buffer. Cells were disrupted by sonication and clear supernatant was collected by centrifuge at 4 °C. Enzyme activities were measured spectrophotometrically in a thermostat (30 °C) recording spectrophotometer (U-2000A, Hitachi Co., Tokyo, Japan). All compounds of the reaction mixture were pipetted into a cuvette with 1 cm light path and reaction was initiated by adding the

cell extract or substrate to give a final volume of 1 ml. The wavelength and the millimolar extinction coefficients for NAD^+, NADH, $NADP^+$ and NADPH were 340 nm and 6.22 l mM^{-1} cm^{-1}. One unit (U) of the specific enzyme activity was defined as the amount of enzyme required to convert 1 μmol of the substrate into the specific product per minute per milligram of protein. The assay conditions for the measurement of enzyme activity were as follows: phosphoglucose isomerase (*pgi*): 0.1 M Tris–HCl (pH 7.8), 10 mM $MgCl_2$, 0.5 mM $NADP^+$, 1 U of glucose-6-phosphate dehydrogenase, 2 mM F-6-P (Salas et al., 1965); hexokinase (*glk*): 0.1 M Tris–HCl (pH 7.5), 60 mM $MgCl_2$, 1 mM DTT, 0.5 mM $NADP^+$, 2 mM ATP, 15 mM glucose, 2 U of glucose-6-phosphate dehydrogenase (Samuelov et al., 1991); triose phosphate isomerase (*tpi*A): 300 mM triethanolamine buffer (pH 7.8), 0.2 mM NADH, 1 U of glycerolphosphate dehydrogenase, 5 mM glyceraldehydes-3-phosphate; 3-phospho-glycerate kinase: 0.1 M triethanolamine buffer (pH 7.8), 1 mM EDTA, 2 mM $MgSO_4 \cdot 7H_2O$, 1 U of glyceraldehydes-phosphate dehydrogenase, 1 mM ATP, 10 mM 3-phosphoglycerate (Sridhar et al., 2000); citrate synthase (*glt*A): 0.1 M Tris–HCl (pH 8.0), 8 mM Acetyl-CoA, 10 mM sodium oxaloacetate, 10 mM DTNB (Parvin, 1969); isocitrate lyase: 0.1 mM potassium phosphate (pH 7.0), 5.0 mM $MgCl_2$, 1.0 mM DTT, 0.3 mM NADH, 5.0 mM isocitrate (Van der Werf et al., 1997); malate dehydrogenase (*mdh*): 2.5 ml of 0.1 M Tris–HCl (pH 8.8), 0.1 ml of 0.1 mM sodium malate, 0.1 ml of 10 mM NAD and cell extract, and water to a final volume of 3 ml (Park et al., 1995b); malic enzyme (*mae*B): 0.1 M Tris–HCl (pH 7.8), 5 mM $MgCl_2$, 0.6 mM NADP, 40 mM malate (Van der Werf et al., 1997); lactate dehydrogenase (*ldh*A): in a total volume of 3 ml containing 300 mmol potassium phosphate, pH 7.0, 2 mmol sodium pyruvate, 0.4 mmol NADH (Van der Werf et al., 1997); glucose-6-phosphate dehydrogenase (*zwf*): 0.1 M Tris–HCl (pH 7.5), 2.5 mM $MnCl_2$ or 6 mM $MgCl_2$, 2 mM glucose-6-phosphate, 1 mM DTT, and 1 mM NAD(P) (Lamed and Zeikus, 1980); overall activity of ED pathway: 0.75 ml of 0.2 M Tris–HCl buffer (pH 7.2) containing 5 mM 6PG, 10 mM $MgSO_4$. After incubation for 30 min, at 30 °C, the reaction was terminated by addition of 0.5 ml of 0.5 M HCl containing 0.02% (w/v) dinitrophenylhydrazine. After an additional 10 min of incubation at room temperature, 1 ml of 2 M NaOH was added, and the absorbance was measured at 450 nm. Pyruvic acid was used as standard (Canonaco et al., 2001); FDP aldolase (*fba*A): 0.05 M Tris–HCl (pH 7.5), 0.1 mM cysteine-hydrochloride, 0.1 M potassium acetate, 2 mM FDP, 0.7 mM $CoCl_2$, 0.25 mM NADH, 20 U of triose phosphate isomerase, 2 U of glyceraldehyde-3-phosphate dehydrogenase (Samuelov et al., 1991).

2.4. RNA preparation and design of PCR primers

Total RNA was isolated from *E. coli* cells by Qiagen RNeasy® Mini Kit (QIAGEN K.K., Japan) according to the manufacturer's recommendations. The quantity and purity of the RNA were determined by optical density measurements at 260 and 280 nm and by 1% formaldehyde agarose gel electrophoresis (data not shown). The sequences of primers for respective genes used in this study are listed in Table 1. Criteria for the design of the gene-specific primer pairs were followed according to Sambrook and Russell (2001). The primers used in this study were synthesized at Hokkaido System Science Co. (Sapporo, Hokkaido, Japan). In all the cases, the primer-supplied company confirmed the absolute specificity of primers. For instance, the *zwf*-specific primer pair was unable to amplify templates derived from any of the other sequences (data not shown).

2.5. cDNA synthesis and PCR amplification

RT-PCR reactions were carried out in a TaKaRa PCR Thermal Cycler (TaKaRa TP240, Japan) using Qiagen® OneStep RT-PCR Kit (QIAGEN K.K., Japan). The reaction mixture was incubated for 30 min at 50 °C for reverse transcription (cDNA synthesis) followed by 15 min incubation at 95 °C for initial PCR activation. Then, the process was subjected to 30 cycles of amplification which consisted of a denaturing step (94 °C for 1 min), an annealing step (approxi-

Table 1
Genes name, used primer pairs, the optimal amount of input template RNA for RT-PCR study after calibration of each gene and amplified PCR products of respective genes in agarose gel

Gene name	Primer pairs	Amplified PCR products (bp)	Input RNA for RT–PCR (ng)		
			E. coli DF11/pAeKG1	*E. coli* DF11	*E. coli* JM109
*dna*A	5′-GTGTCACTTTCGCTTTGGCA-3′ 5′-TTACGATGACAATGTTCTGA-3′	1385	2.8	4.4	4.1
pgi	5′-AACATCAATCCAACGCAGACC-3′ 5′-GCCACGCTTTATAGCGGTTAA-3′	1635	5.7	8.8	8.2
zwf	5′-ATGGCGGTAACGCAAACA-3′ 5′-AACTCATTCCAGGAACGACCA-3′	1465	11.4	17.6	16.4
edd	5′-TGAATCCACAATTGTTAC-3′ 5′-AAAAAGTGATACAGGTTG-3′	1800	1.4	2.2	2.1
eda	5′-TGGAAAACAAGTGCAGAATCA-3′ 5′-TTAGCGCCTTCTACAGCTTCA-3′	621	5.7	8.8	8.2
*pyk*A	5′-GCTTCGCAGAACAAAAATCG-3′ 5′-ACCGTTAAAATACGCGTGGT-3′	1436	0.7	1.1	1.1
*pps*A	5′-ATGTCCAACAATGGCTCGT-3′ 5′-TTCTTCAGTTCAGCCAGGCTT-3′	2371	11.4	2.2	32.8
*ldh*A	5′-CTCGCCGTTTATAGCACAAA-3′ 5′-TTAAACCAGTTCGTTCGGGCA-3′	983	1.4	8.8	8.2
pta	5′-TTATGCTGATCCCTACCGGAA-3′ 5′-TGCTGCTGTGCAGACTGAAT-3′	2125	0.7	4.4	16.4
*ack*A	5′-GTACTGGTTCTGAACTGCGG-3′ 5′-CTCGCGTCTTGCGCGATAA-3′	1170	5.7	2.2	2.1
*lpd*A	5′-AAATCAAAACTCAGGTCGTGG-3′ 5′-TTCTTCTTCGCTTTCGGGTT-3′	1409	2.8	1.1	8.2
*ace*E	5′-TTTCCCAAATGACGTGGATC-3′ 5′-GCGGGTTAACTTTATCTGCA-3′	2640	1.4	1.1	1.1
*ace*F	5′-CGAAATCAAAGTACCGGACA-3′ 5′-TTACATCACCAGACGGCGAAT-3′	1882	5.7	8.8	2.1
*glt*A	5′-CAAAAGCAAAACTCACCCTCA-3′ 5′-TCGCTTTTAAAGTCGCGTT-3′	1258	1.4	17.6	8.2
icd	5′-AAGTAGTTGTTCCGGCACAAG-3′ 5′-ATGTTTTCGATGATCGCGTC-3′	1230	2.8	35.1	1.1
*ace*A	5′-ATGAAAACCCGTACACAACAA-3′ 5′-AACTGCGATTCTTCAGTGGA-3′	1300	0.7	1.1	32.8
*ace*B	5′-AGGCAACAACAACCGATGAA-3′ 5′-TTACGCTAACAGGCGGTAGC-3′	1590	11.4	8.8	8.2
*mae*B	5′-ATGGATGACCAGTTAAAA-3′ 5′-TTACAGCGGTTGGGTTTG-3′	2271	5.7	1.1	16.4
ppc	5′-CGAACAATATTCCGCATTGC-3′ 5′-TATTACGCATACCTGCCGCAA-3′	2633	1.4	2.2	2.1
*pck*A	5′-TGCGCGTTAACAATGGTTTG-3′ 5′-TTACAGTTTCGGACCAGCC-3′	1619	2.8	8.8	8.2
*phb*A	5′-AATTGTATCTGCTGCTCGGA-3′ 5′-TTTACGTTCGACTGCCAGCG-3′	1160	5.7	4.4	8.2
*phb*B	5′-ATGACCGATGTCGTGATT-3′ 5′-CTTGCGCTCTACCGCTAGG-3′	1151	11.4	2.2	16.4
*phb*C	5′-ATGGCGACAGGTAAGGGCGC-3′ 5′-CGCTTTGGCCTTAACGTAG-3′	1737	1.4	1.1	2.1
*pnt*A	5′-TGCGAATTGGCATACCAAGA-3′ 5′-GAACATTTTCAGCATGCGCT-3′	1517	5.7	1.1	8.2
*udh*A	5′-ATTGGTAAAGCAGGGGGCA-3′	1313	0.7	8.8	1.1

Table 1 (*Continued*)

Gene name	Primer pairs	Amplified PCR products (bp)	Input RNA for RT–PCR (ng)		
			E. coli DF11/pAeKG1	*E. coli* DF11	*E. coli* JM109
gnd	5′-GGTTAAGGCCGTTTAAAGCG-3′ 5′-AAGCAACAGATCGGCGTAGT-3′ 5′-TAATCCAGCCATTCGGTATG-3′	1389	11.4	17.6	2.1
pfk A	5′-AAATCGGTGTGTTGACAAGC-3′ 5′-AGTTTTTTCGCGCAGTCCA-3′	941	1.4	35.1	8.2
pfk B	5′-TATACGTTGACACTTGCGCC-3′ 5′-TAGCGGGAAAGGTAAGCGTAA-3′	915	0.7	1.1	1.1
fba A	5′-TGATTTCGTAAAACCTGGCG-3′ 5′-ATCGCGTTCAGTTCCTGGAAT-3′	1045	5.7	4.4	8.2
gap A	5′-GTAGGTATCAACGGTTTTGGC-3′ 5′-TTTGGAGATGTGAGCGATCA-3′	975	2.8	8.8	16.4
gap C	5′-TGGTATTAACGGTTTTGGTCG-3′ 5′-TAGCGAATTTTTCGAGGGTG-3′	980	1.4	17.6	2.1
tpi A	5′-TGCGACATCCTTTAGTGATGG-3′ 5′-TTAAGCCTGTTTAGCCGCTT-3′	765	5.7	2.2	8.2
pgk	5′-AGATGACCGATCTGGATCTTG-3′ 5′-CTCTTCGAGCATCGCTACTG-3′	1131	1.4	8.8	8.2
eno	5′-TCGTAAAAATCATCGGTCGTG-3′ 5′-TTATGCCTGGCCTTTGATCT-3′	1284	2.8	1.1	16.4
gpm A	5′-AAGCTGGTTCTGGTTCGTCAT-3′ 5′-ACTTCGCTTTACCCTGGTTT-3′	735	0.7	2.2	2.1
gpm B	5′-TAGTCCGCCACGGTGAAA-3′ 5′-TGCAGCTCATCTAATGCAGG-3′	619	11.4	8.8	8.2
pyk F	5′-CCAAAATTGTTTGCACCATCG-3′ 5′-ACGTGAACAGATGCGGTGTTA-3′	1390	5.7	4.4	1.1
rpi A	5′-TGACGCAGGATGAATTGAA-3′ 5′-TCACAATGGTTTTGACACCG-3′	650	1.4	2.2	2.1
rpe	5′-TTTGATTGCCCCCTCAATTC-3′ 5′-TTACCTTTGCCAGTTCACTGC-3′	649	1.4	1.1	8.2
tkt A	5′-TCACGTAAAGAGCTTGCCAAT-3′ 5′-CTTTTGCTTTCGCAACAACG-3′	2000	5.7	1.1	1.1
tkt B	5′-CCGAAAAGACCTTGCCAAT-3′ 5′-TTTCACTCCCAGCACCTTATG-3′	1978	0.7	2.2	8.2
tal A	5′-AGACGGCATCAAACAGTTCA-3′ 5′-ATAGTTTGGCGGCAAGAAGA-3′	931	11.4	8.8	16.4
tal B	5′-ACAAATTGACCTCCCTTCGT-3′ 5′-AGCAGATCGCCGATCATTTT-3′	940	2.8	4.4	2.1
pfl A	5′-TTGGTCGCATTCACTCCTTT-3′ 5′-CCTTATGACCGTACTGCTCAA-3′	715	5.7	2.2	8.2
pfl D	5′-TCGTATCTCTCGCCTCAAAA-3′ 5′-TTACAGCTGATGCGCTGTCC-3′	2285	5.7	1.1	8.2
suc A	5′-TTTGAAAGCCTGGTTGGACTC-3′ 5′-TCAGCGCGTCATTAACCAGAT-3′	2757	2.8	1.1	16.4
sdh C	5′-ATGTGAAAAAACAAAGACCTG-3′ 5′-TCCTGCGAGAAGTGAAAGCA-3′	360	1.4	8.8	2.1
frd A	5′-TTCAAGCCGATCTTGCCAT-3′ 5′-CCATTCGCCTTCTCCTTCTTA-3′	1791	5.7	17.6	8.2
acn A	5′-TACGAGAAGCCAGTAAGGACA-3′ 5′-ACGAATGACATAATGCAAA-3′	2643	1.4	35.1	8.2
acn B	5′-TACCGTAAGCACGTAGCTGAG-3′ 5′-AACCGCAGTCTGGAAAATCA-3′	2580	2.8	1.1	16.4

Table 1 (*Continued*)

Gene name	Primer pairs	Amplified PCR products (bp)	Input RNA for RT–PCR (ng)		
			E. coli DF11/pAeKG1	*E. coli* DF11	*E. coli* JM109
fum A	5′-CAAACCCTTTCATTATCAGGC-3′ 5′-TATTTCACACAGCGGGTGCAT-3′	1631	0.7	4.4	2.1
mdh	5′-ATGAAAGTCGCAGTCCTCGG-3′ 5′-ATTAACGAACTCTTCGCCCA-3′	927	11.4	8.8	8.2
glk	5′-TGCATTAGTCGGTGATGTGG-3′ 5′-TGACCTAAGGTCTGGCGTAAA-3′	941	5.7	17.6	1.1
pts G	5′-GAATGCATTTGCTAACCTGCA-3′ 5′-CGGATGTACTCATCCATCTCG-3′	1410	1.4	2.2	2.1
pts H	5′-AAGTTACCATTACCGCTCCGA-3′ 5′-TTCCGCCATCAGTTTAACCA-3′	231	1.4	1.1	8.2
cya A	5′-TTGAGACTCTGAAACAGAGAC-3′ 5′-ATTGCTGTAATAGCGGCGTA-3′	2520	5.7	2.2	1.1
crp	5′-TGCTTGGCAAACCGCAAA-3′ 5′-TTAACGAGTGCCGTAAACGA-3′	621	0.7	8.8	8.2
fru R	5′-AAACTGGATGAAATCGCTCG-3′ 5′-TTAGCTACGGCTGAGCACG-3′	999	11.4	4.4	16.4
fnr	5′-AGCGAATTATACGGCGCATT-3′ 5′-AGGCAACGTTACGCGTATGA-3′	735	2.8	2.2	2.1
arc A	5′-CAGACCCCGCACATTCTTATC-3′ 5′-TAATCTTCCAGATCACCGCA-3′	710	5.7	1.1	8.2
dna K	5′-AATAATTGGTATCGACCTGGG-3′ 5′-TTGACTTCTTCAAATTCAGCG-3′	1895	5.7	1.1	8.2
dna J	5′-GGCTAAGCAAGATTATTACGA-3′ 5′-GGGTCAGGTCGTCAAAAAACT-3′	1121	22.7	2.2	16.4
grp E	5′-AAGAACAGAAAACGCCTGAGG-3′ 5′-TTTCGCTACAGTAACCATCGC-3′	569	0.7	8.8	2.1
gro L	5′-CGTAAAATTCGGTAACGACGC-3′ 5′-TTACATCATGCCGCCCAT-3′	1630	5.7	4.4	8.2
gro S	5′-TATTCGTCCATTGCATGATCG-3′ 5′-ACGCTTCAACAATTGCCAGA-3′	285	2.8	2.2	8.2
htp G	5′-GAAAGGACAAGAAACTCGTGG-3′ 5′-AAACCAGCAGCTGGTTCATA-3′	1865	11.4	1.1	16.4
lon	5′-TCTGAACGCATTGAAATCCC-3′ 5′-TTTGCAGTCACAACCTGCAT-3′	2331	0.7	1.1	2.1
ibp A	5′-TTTATCCCCGCTTTACCGTT-3′ 5′-TTAGTTGATTTCGATACGGCG-3′	398	22.7	17.6	8.2
ibp B	5′-TCGATTTATCCCCACTGATGC-3′ 5′-TTAGCTATTTAACGCGGGACG-3′	415	2.8	35.1	1.1
sec A	5′-TGTTAACTAAAGTTTTCGG-3′ 5′-CATGGCACTGCTTGTATTTT-3′	2675	5.7	1.1	1.1
lep B	5′-TTTGCCCTGATTCTGGTGATT-3′ 5′-TTAATGGATGCCGCCAATG-3′	961	1.4	4.4	2.1
dsb A	5′-ATGAAAAAGATTTGGCTGGCG-3′ 5′-CTCGGACAGATATTTCACTG-3′	612	0.7	8.8	8.2
rpo D	5′-AGCAAAACCCGCAGTCACA-3′ 5′-AAGCTACGCAGCACTTCAGAA-3′	1821	0.7	17.6	1.1
rpo E	5′-TGAGCGAGCAGTTAACGGA-3′ 5′-GCCTGATAAGCGGTTGAACTT-3′	567	11.4	2.2	8.2
rpo H	5′-GCAAAGTTTAGCTTTAGCCCC-3′ 5′-CAATGGCAGCACGCAATTTT-3′	830	2.8	1.1	16.4
rpo S	5′-GTCAGAATACGCTGAAAGTTC-3′	978	5.7	2.2	2.1

Table 1 (*Continued*)

Gene name	Primer pairs	Amplified PCR products (bp)	Input RNA for RT–PCR (ng)		
			E. coli DF11/pAeKG1	*E. coli* DF11	*E. coli* JM109
	5′-GAACAGCGCTTCGATATTCA-3′				
*usp*A	5′-AAACACATTCTCATCGCGGT-3′	423	5.7	8.8	8.2
	5′-TTATTCTTCTTCGTCGCGCA-3′				
*usp*B	5′-CGTCGCATTATTTTGGGCT-3′	311	22.7	4.4	8.2
	5′-TCATCAATGCAATCAGGCTG-3′				
*adh*E	5′-ATGTCGCTGAACTTAACGCA-3′	2655	0.7	2.2	16.4
	5′-GCGGATTTTTTCGCTTTTTTC-3′				
*fdh*F	5′-AAAAAGTCGTCACGGTTTGC-3′	2125	5.7	1.1	2.1
	5′-TTCGCGCAGGCGAGTTTT-3′				
*rps*A	5′-GCTCAACTCTTTGAAGAGTC-3′	1650	2.8	2.2	8.2
	5′-TCGCCTTTAGCTGCTTTGAA-3′				
*tuf*A	5′-TTTGAACGTACAAAACCGCA-3′	1159	11.4	8.8	1.1
	5′-AGAACTTTAGCAACAACGCCC-3′				
*fpk*A	5′-TAAAGTAACGCTGCTGGCGA-3′	790	0.7	4.4	1.1
	5′-TTTAGCAGAATCTGCGGCTT-3′				
*gre*A	5′-ATGCAAGCTATTCCGATGAC-3′	471	22.7	2.2	2.1
	5′-CAGGTATTCCACCTTAATTAC-3′				
*fab*D	5′-TTGCATTTGTGTTCCCTGGA-3′	900	2.8	1.1	8.2
	5′-CTGCCATCGCTGAAGGTT-3′				
*pot*D	5′-AAAAAATGGTCACGCCACCT-3′	1039	5.7	1.1	4.1
	5′-AACGTCCTGCTTTCAGCTTCT-3′				

mately 5 °C below melting temperature, T_m, of primers for 1 min) and an extension step (72 °C for 1 min), and finally the reaction mixture was for 10 min at 72 °C for final extension. To check for nucleic acid contamination, one negative control was run in every round of RT-PCR. This control lacks the template RNA in order to detect possible contamination of the reaction components. 5 μl of amplified products were run on a 2% agarose gel. Gels were stained with 1 μg ml^{-1} of ethidium bromide, photographed using a Digital Image Stocker (DS-30, FAS III, Toyobo, Osaka, Japan) under UV light and analyzed using Gel-Pro Analyzer 3.1 (Toyobo, Osaka, Japan) software. Although the PCR products obtained for all the genes showed the predicted sizes on agarose gel, the identity of amplified fragments of some genes was demonstrated by DNA sequencing (data not shown). In order to determine the optimal amount of input RNA, the twofold diluted template RNA was amplified in RT-PCR assays under identical reaction conditions to construct a standard curve for each gene product. When the optimal amount of input RNA was determined for each gene product, RT-PCR was carried out under identical reaction conditions to detect differential transcript levels of genes. The gene *dna*A, which encodes *E. coli* DNA polymerase and is not subjected to variable expression, i.e. abundant expression at relatively constant rates in most cells, was used as an internal control in the RT-PCR determinations. To calculate the standard deviation, RT-PCR study of each gene was independently performed three times under identical reaction condition.

3. Results

Batch cultures of *E. coli* JM109, *pgi* knockout *E. coli* DF11, and recombinant *pgi* knockout *E. coli* DF11/pAeKG1 having *phb* genes were conducted in LB medium containing 20 g l^{-1} glucose where dissolved oxygen (DO) concentration and pH were maintained at about 3 and 7 ppm with the aid of computer control, respectively. Fig. 1 shows the batch experimental results for those three strains. Table 2 shows the specific growth rate, specific glucose consumption rate, soluble protein

concentration and acetic acid concentration at the time shown by arrow in Fig. 1 for RT-PCR analysis. The PHB concentration and PHB content obtained from *E. coli* DF11/pAeKG1 at the time of RT-PCR analysis were 0.63 g l^{-1} (see Fig. 1c) and 10.71%, respectively. The enzyme activities of *pgi* at those times were 0.417 ± 0.01, 0.019 ± 0.018 and 0.024 ± 0.024 U mg^{-1} protein for *E. coli* JM109, *E. coli* DF11 and *E. coli* DF11/pAeKG1, respectively, indicating the complete inactivation of phosphoglucose isomerase for the latter two. Figs. 1a and b show that the cell growth of *pgi* knockout *E. coli* DF11 was repressed as compared with that of *E. coli* JM109. The cell growth was recovered to some extent as shown in Fig. 1c when NADPH absorbing pathway such as PHB synthetic pathway was included.

A total of 87 *E. coli* genes involved in central metabolic pathways and key regulatory mechanisms were chosen for studying differential gene expression in *pgi* mutant *E. coli*. In order to determine the optimal amount of input RNA, the twofold diluted template RNA were amplified in the RT-PCR assays with identical reaction conditions to construct a standard curve for each gene product. As an example, the standard curve for the gene *rpe* was shown in Fig. 2 and the optimal amounts of input RNA were determined for each gene product by this way, and are listed in Table 1. The RT-PCR analysis of each gene was performed three times independently with identical reaction condition and the standard deviations were calculated. Most of the genes showed relatively small standard deviations (less than 0.05). However, larger standard deviations (about 0.13) were found in some genes such as *edd*, *tpi*A, *tkt*A, *gro*L, *fnr*, *lep*B, *usp*A and *rpo*E. Some of the gene expressions for *E. coli* JM109 are shown in Fig. 3. A number of significant changes in differential gene expressions obtained by semi-quantitative RT-PCR analysis were observed in *pgi* mutant *E. coli* DF11 and in recombinant *pgi* mutant *E. coli* DF11/pAeKG1 having *phb* genes as compared with those in *E. coli* JM109, and the results are shown in Figs. 4 and 5, respectively, where the values shown in the figures are the ratios of the gene expressions as compared with the corresponding gene expressions of *E. coli* JM109.

3.1. Glycolysis and pentose phosphate pathway genes

Figs. 4 and 5 show that the glycolysis and pentose phosphate (PP) pathway genes were affected significantly by expression of *phb* genes in *pgi* mutant *E. coli* DF11/pAeKG1 as well as in *pgi* mutant *E. coli* DF11 without *phb* genes. The results show that the transcript abundance of several glycolytic genes such as *pfk*A, *fba*A, *tpi*A, *gap*A, *pgk*, *eno*, *pyk*A, *pps*A and *pck*A were increased 1.5–12.9-fold in recombinant *pgi* mutant *E. coli* DF11/pAeKG1 having *phb* genes compared to those in control *E. coli* JM109 (see Fig. 4). Since the first six of those genes catalyze reversible reactions, their upregulation enhances the flux in the glycolytic direction, which is much greater than the gluconeogenic flux during growth in glucose. The downregulation of *pyk*F in both *E. coli* DF11 and *E. coli* DF11/pAeKG1, but not *pyk*A (Figs. 4 and 5) suggests that these two isoenzymes were differentially regulated. Indeed, *pyk*F, but not *pyk*A, has been regarded to be negatively regulated by *fru*R (Saier and Ramseier, 1996), a global regulatory gene that was found to be upregulated in both *E. coli* DF11 and *E. coli* DF11/pAeKG1. Interestingly, however, *pps*A (coding for phosphoenol pyruvate synthase) was upregulated 12.9-fold in *E. coli* DF11/pAeKG1 but was almost unchanged in *E. coli* DF11 compared to those in *E. coli* JM109.

Among the pentose phosphate pathway genes, most of the gene transcripts in both *E. coli* DF11 and *E. coli* DF11/pAeKG1 were upregulated except *gnd* gene compared to those in *E. coli* JM109 (Figs. 4 and 5). The expression of *gnd* (coding for 6-phosphogluconate dehydrogenase), which is regulated by the growth rate (Pearse and Wolf, 1994), was clearly decreased in *pgi* mutants as the growth rate reduced as compared with that of *E. coli* JM109 (see Table 2). By contrast, *tal*A (coding for transaldolase A) was upregulated in *pgi* mutant *E. coli*, although *tal*B, the isoenzyme of *tal*A, showed no change. In addition, *edd* was upregulated in both *pgi* mutants, although *eda* was downregulated significantly as was shown in Figs. 4 and 5.

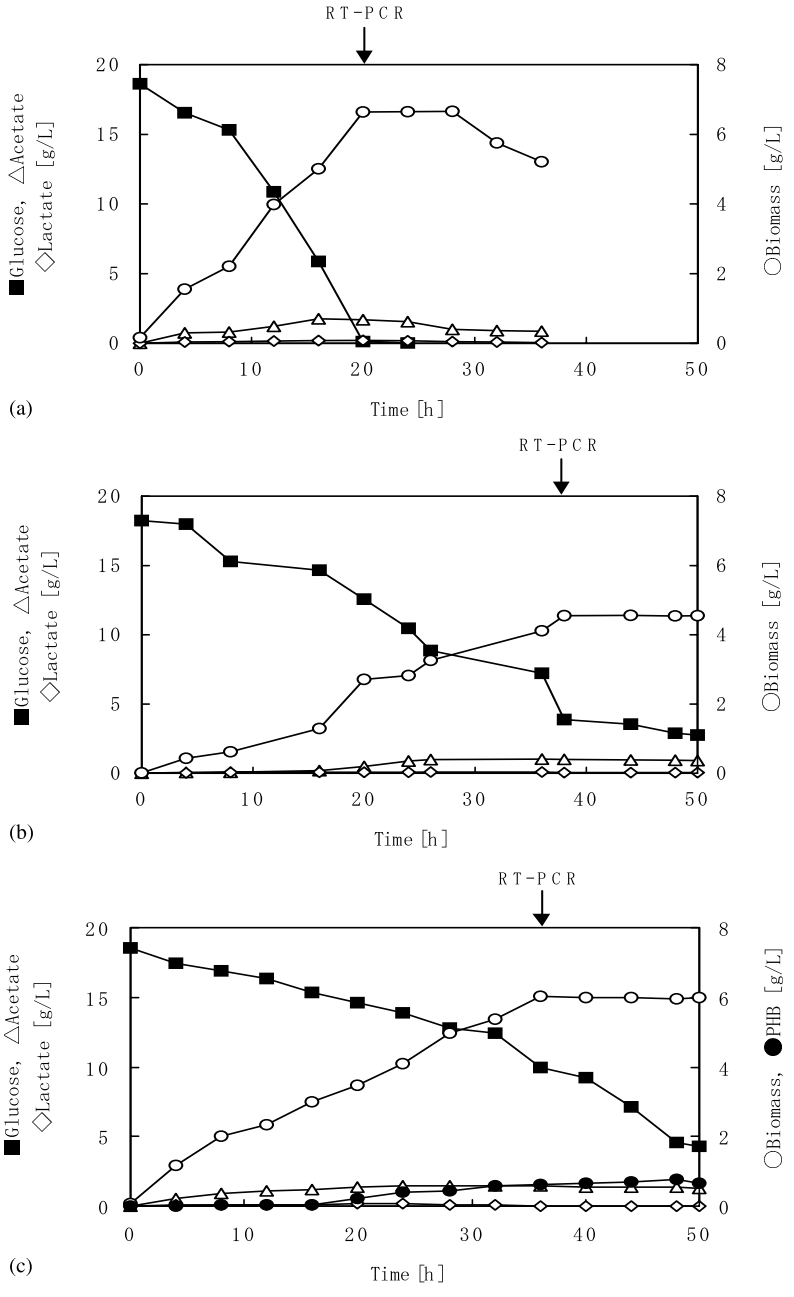

Fig. 1. Batch experimental results of (a) *E. coli* JM109, (b) *E. coli* DF11 and (c) *E. coli* DF11/pAeKG1. The arrow indicates the sampling time for RT-PCR analysis.

3.2. Fermentation and TCA cycle genes

Most of the TCA cycle genes were downregulated except *icd*A in both *pgi* mutants *E. coli* compared to those in *E. coli* JM109. This downregulation was expected since most of the TCA cycle genes such as *glt*A (Park et al., 1994), *suc*A (Park et al., 1997), *sdh*C (Park et al., 1995a), *fum*A

Table 2
Comparison of specific growth rate, specific glucose consumption rate, extracted soluble protein, and acetate concentrations at the time of harvesting for semi-quantitative RT-PCR analysis

Strain	Specific growth rate (h^{-1})[a]	Specific glucose consumption rate[a] (mmol g^{-1} cell h^{-1})	Soluble protein[a] (mg ml^{-1})	Acetate[a] (g l^{-1})
DF11/ pAeKG1	0.016±0.001	0.37±0.02	2.21±0.03	1.42±0.02
DF11	0.011±0.001	0.56±0.01	1.61±0.01	1.0±0.03
JM109	0.035±0.002	0.61±0.03	1.05±0.03	1.69±0.01

[a] Standard deviations from duplicate experiments.

(Park and Gunsalus, 1995) and *mdh* (Park et al., 1995b) are known to be regulated by several regulators such as *fnr* and *arc*A that were found to be upregulated in both *pgi* strains. The upregulation of *icd*A may be due to the positive regulation of *fru*R (Saier and Ramseier, 1996).

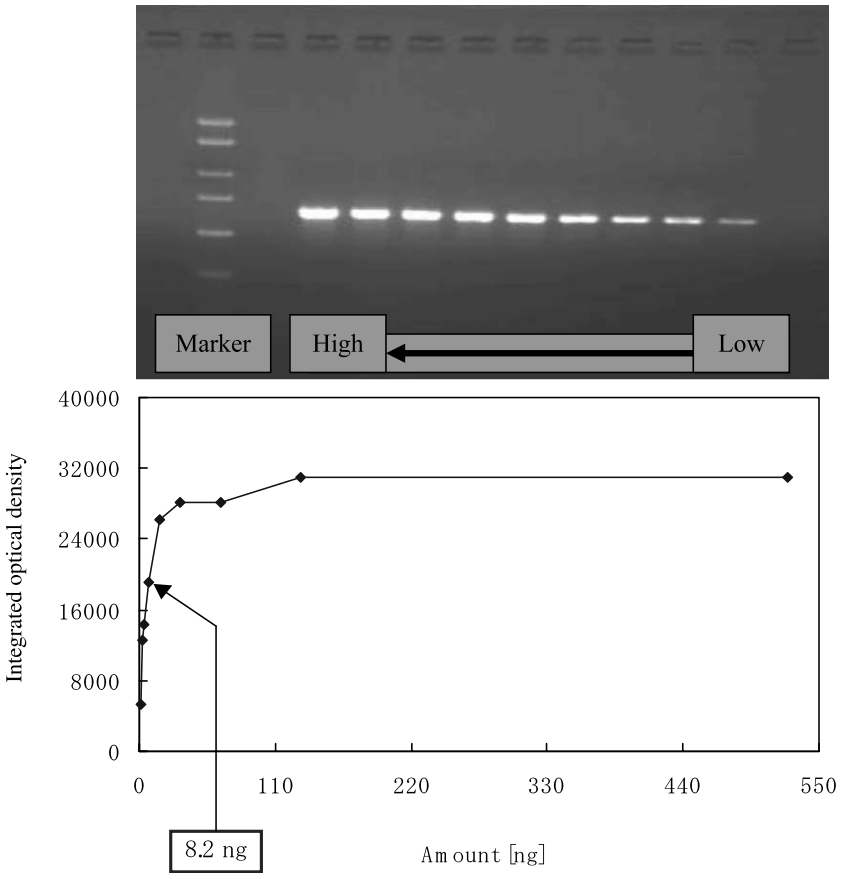

Fig. 2. The standard curve of semi-quantitative RT-PCR analysis of *rpe* transcripts that was constructed by amplifying the twofold diluted template RNA. RT-PCR products were run in 2% agarose gel and the signals were calculated by Gel-Pro Analyzer 3.1 software. The arrow indicates the amount of input RNA chosen for semi-quantitative RT-PCR analysis of *rpe* transcripts.

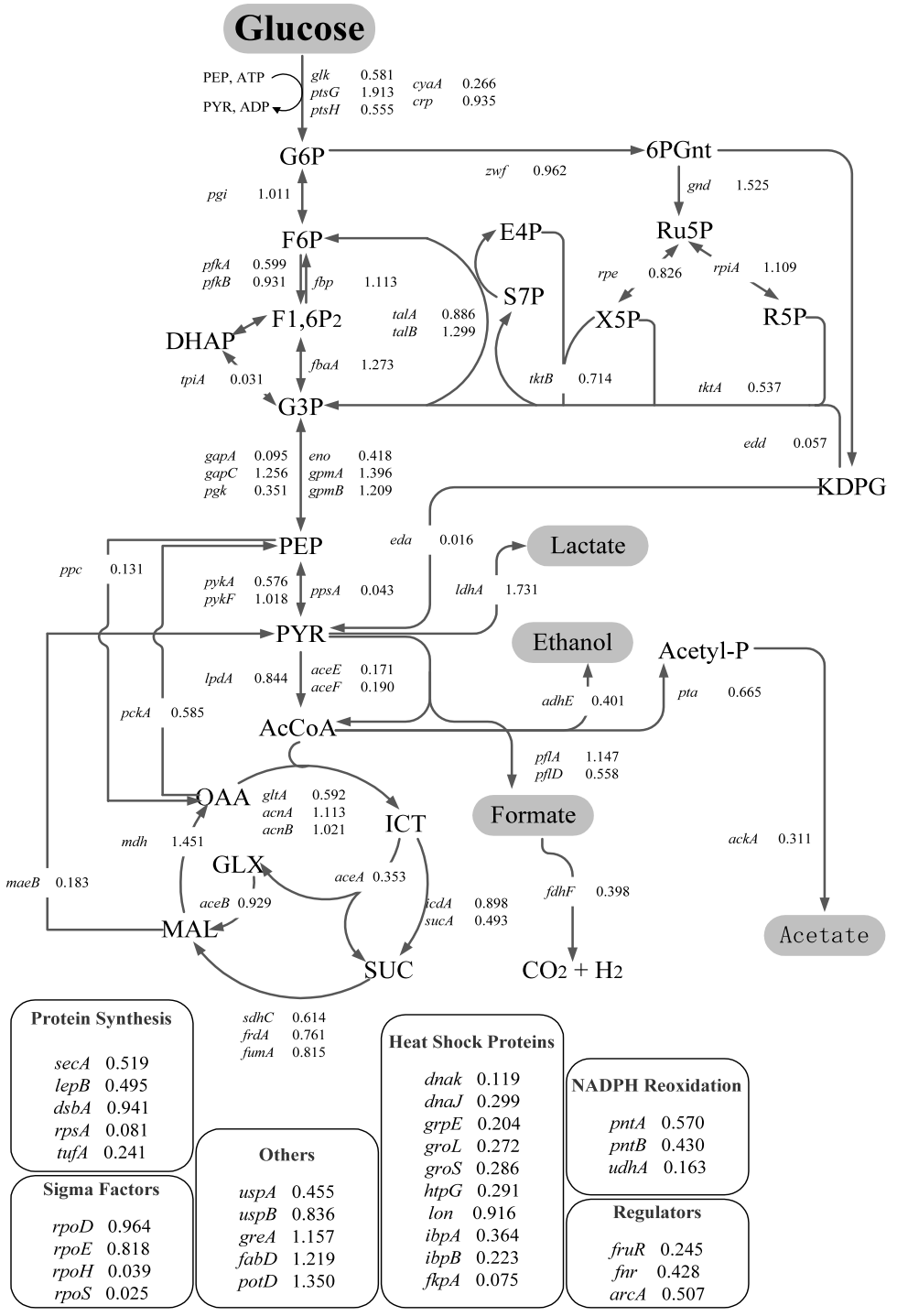

Fig. 3. The transcript levels of central metabolic pathway genes for *E. coli* JM109. Symbols for genes inside the boxes follow the *E. coli* K-12 linkage map. The abbreviations for the metabolites are given Appendix A.

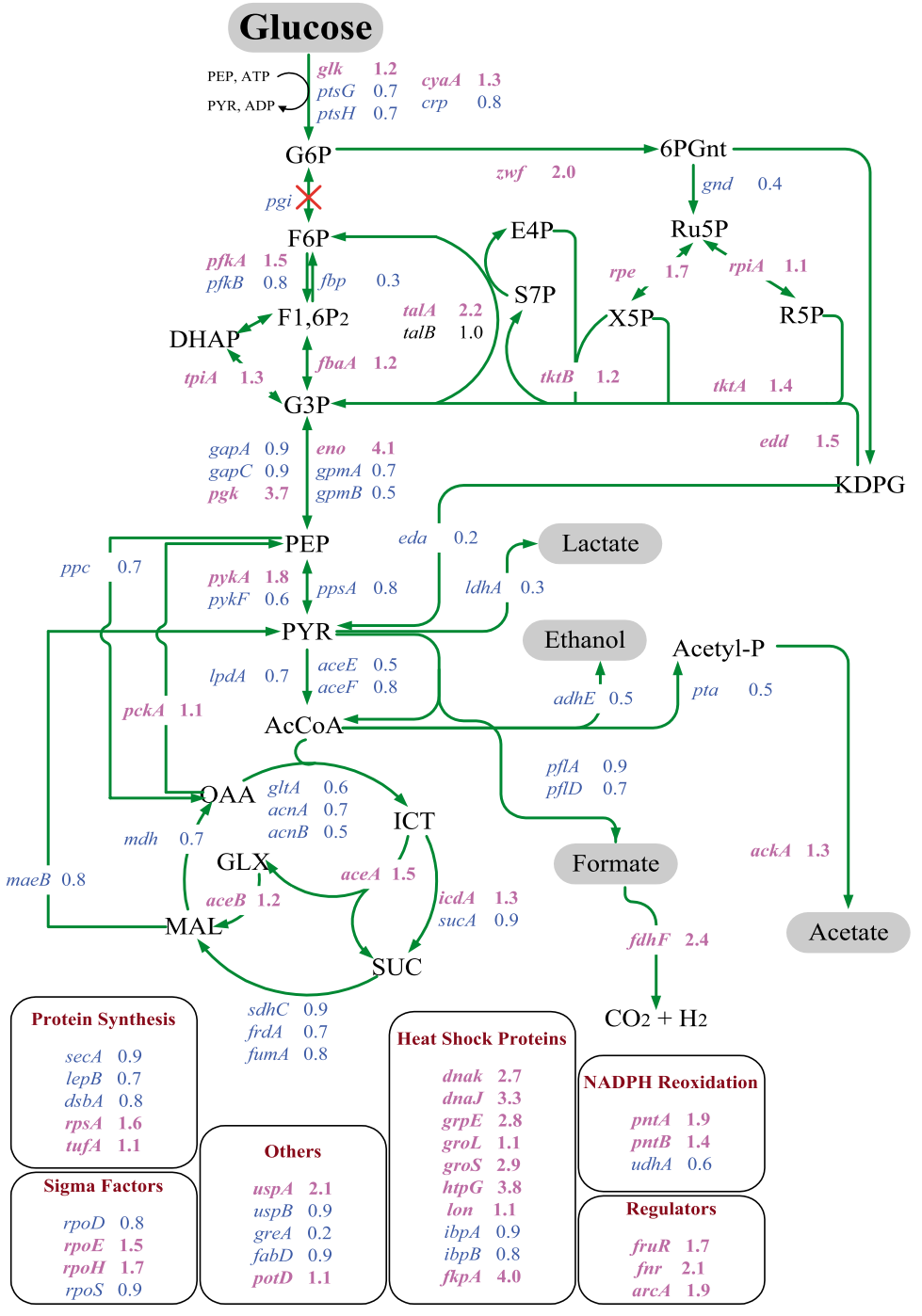

Fig. 4. The transcript levels of central metabolic pathway genes for *E. coli* DF11 relative to those in *E. coli* JM109. Symbols for genes inside the boxes follow the *E. coli* K-12 linkage map. Pink color represents upregulation, blue represents downregulation, and black represents no change. The abbreviations for the metabolites are given in Appendix A.

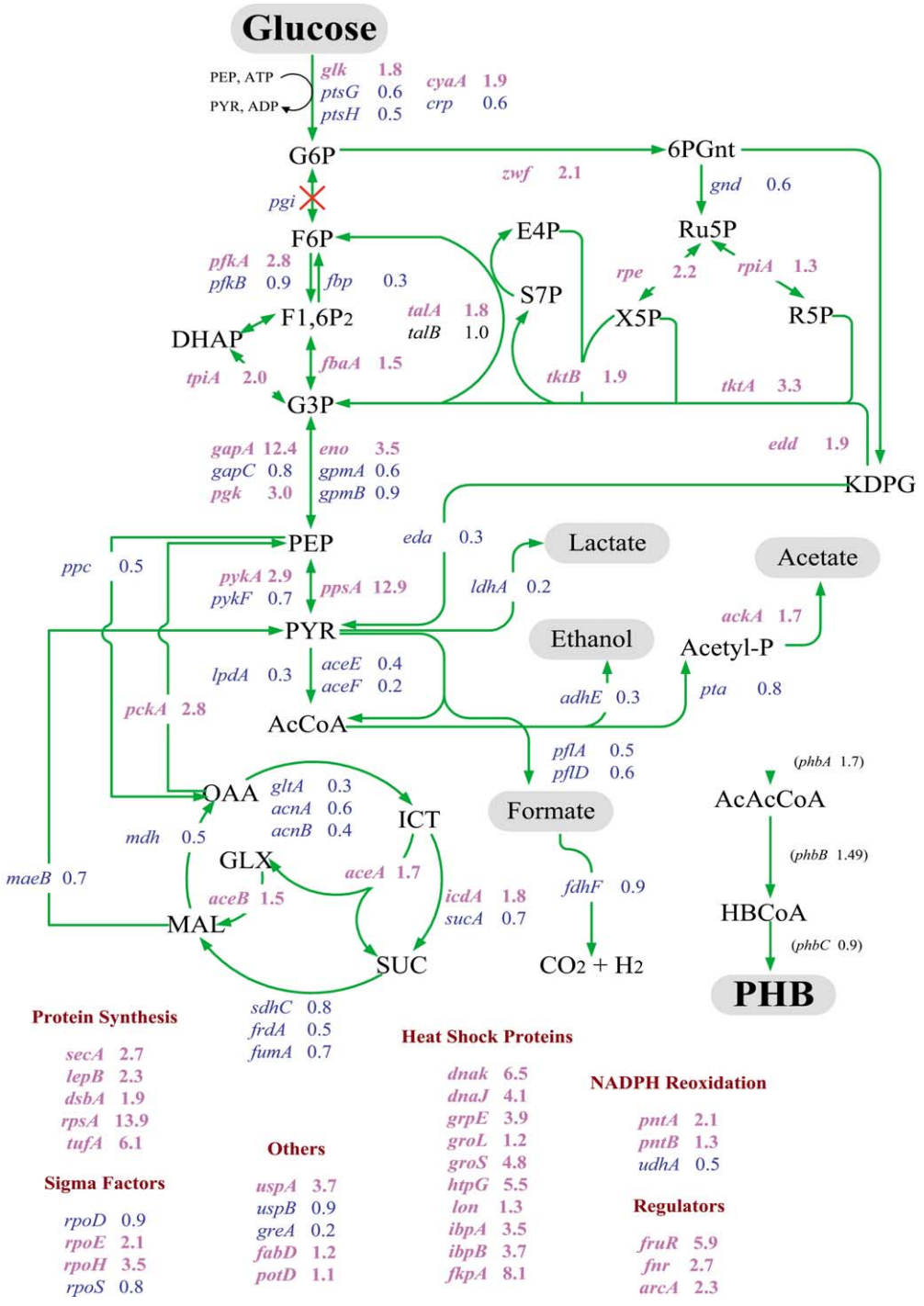

Fig. 5. The transcript levels of central metabolic pathway genes for *E. coli* DF11/pAeKG1 relative to those in *E. coli* JM109. Symbols for genes inside the boxes follow the *E. coli* K-12 linkage map. Pink color represents upregulation, blue represents downregulation, and black represents no change. The *phb* genes in parentheses are not normalized. The abbreviations for the metabolites are given in Appendix A.

In addition, the genes involved in the glyoxylate shunt (*ace*A and *ace*B) were upregulated in both *pgi* mutants *E. coli* indicating the shortage of C_4 metabolites such as oxaloacetate and thus need to activate the anaplerotic pathway as mentioned in relation to *ppc* gene.

Among the fermentative genes, *fdh*F, coding for formyl dehydrogenase, was increased in *E. coli* DF11, but not in *E. coli* DF11/pAeKG1, compared to that in *E. coli* JM109. The upregulation of *ack*A in both *pgi* mutants is of interest. *Pta* and *ack*A genes were thought to be involved in both acetate synthesis and consumption, and constitutively expressed in the cell (Brown et al., 1977). The upregulation of *ack*A in *pgi* mutants indicates that although both genes are present in the same operon, they are regulated differentially through different promoters. The *pfl*A, *pfl*D, *ldh*A and *adh*E transcripts were downregulated in both *pgi* mutants *E. coli* compared to those in *E. coli* JM109 (Figs. 4 and 5).

3.3. Heat shock and regulatory genes

Metabolically engineered *E. coli* undergoes a variety of physiological changes upon accumulation of PHB, which is not a normal metabolite of *E. coli* and it is considered as a stress on the cells inducing heat shock response. Therefore, the transcript levels of many heat shock proteins such as *dna*K, *dna*J, *gro*S, *grp*E, *htp*G, *ibp*A, and *ibp*B were all upregulated significantly in recombinant *pgi* mutant *E. coli* DF11/pAeKG1 compared to those in *E. coli* JM109 (Fig. 5). Moreover, although those heat shock genes except *ibp*A and *ibp*B were also found to be upregulated in *E. coli* DF11 (see Fig. 4), the level of expression varied among the heat shock genes. Furthermore, the transcript level of *gro*L and *lon* were slightly upregulated in both *pgi* mutants *E. coli*.

The expression level of the genes for the protein secretion and disulfide bond formation, *sec*A, *lep*B and *dsb*A, were increased significantly in *E. coli* DF11/pAeKG1 (Fig. 5) compared to those in *E. coli* JM109 (Fig. 3). This result implies that PHB accumulation in *pgi* mutant *E. coli* increases the activity for protein secretion and disulfide bond formation. The expression ratio of the translation elongation factor gene *tuf*A was significantly higher in *E. coli* DF11/pAeKG1 compared to those in *E. coli* JM109, which was consistent with their coordinated regulation with the ribosomal protein gene *rps*A (Grunberg-Manago, 1996). Expression of *usp*A (coding for universal stress protein) was upregulated in both *pgi* mutants *E. coli*, whereas the expression of *usp*B was almost unchanged compared to those in *E. coli* JM109.

3.4. Relationship between gene expression and enzyme activities

Since the cell's physiological state is dictated at the protein level, mRNA expression results should be complemented by the enzyme activities to provide a better understanding of the observed phenomenon considering that the enzymatic regulations and transcriptional regulations are different. The semi-quantitative RT-PCR results reflect the relative abundance of the transcript, which is influenced by both transcriptional activity and the mRNA stability. In contrast, the activity of enzymes can be regulated by reversible binding of effectors, covalent modification and alteration of enzyme concentration. However, to a large extent, the mRNA expression level reflects the enzyme activity (Martin, 1987). To check how gene expression and enzyme activities correlate with each other, enzyme activities of *glk*, *zwf*, *tpi*A, *fba*A, *ldh*A, *glt*A, *ace*A, *mdh* and *mae*B were measured. Fig. 6 shows the comparison of enzyme activities and gene expressions for three strains. Fig. 7 shows how those are correlated except for *ace*A, where computation of Pearson product moment correlation yields a value of 0.81. Those results show that gene expression data obtained by semi-quantitative RT-PCR were reasonably consistent with the data obtained from enzyme activities except for the gene *ace*A indicating a different level of regulation for that gene after transcription initiation. This phenomenon indicated that *ace*A was expressed in gene level but glyoxylate pathway enzyme was not active for *E. coli* JM109, while it became active for *pgi* mutants.

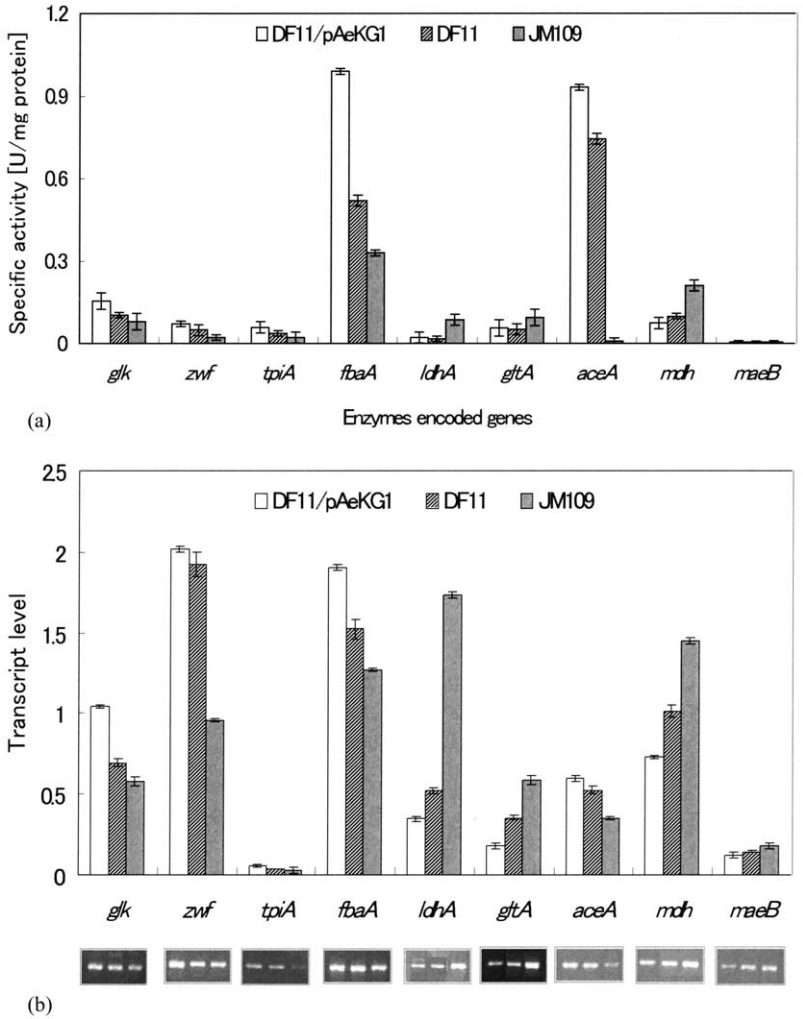

Fig. 6. The measurement of enzyme activities (a) and the mRNA transcript levels obtained from RT-PCR analysis (b). The error bars represent the standard deviations from three measurements.

4. Discussion

The gene *glk* (coding for glucokinase) was upregulated by 1.8- and 1.2-fold in *E. coli* DF11 and *E. coli* DF11/pAeKG1, respectively, while the glucose phosphotransferase system (PTS) genes *pts*G and *pts*H were downregulated compared to those in *E. coli* JM109 (Figs. 4 and 5). The decreases in the *pts*G and *pts*H transcript levels were consistent with the reduced specific glucose consumption rates (Table 2). The increase in *glk* transcript level corroborates a previous report which shows that glucokinase takes over the major role (from the glucose-PTS) to supply glucose-6-phosphate under increased protein synthesis conditions (Arora and Pedersen, 1995), although the mechanism for this induction is still unknown. METAFoR analysis by NMR has shown that a minor fraction of glucose catabolism occurs via ED (Entner-Doudoroff) pathway in both wild type and *pgi* mutant strain. Examination of the operational catabolic pathways and their flux ratios

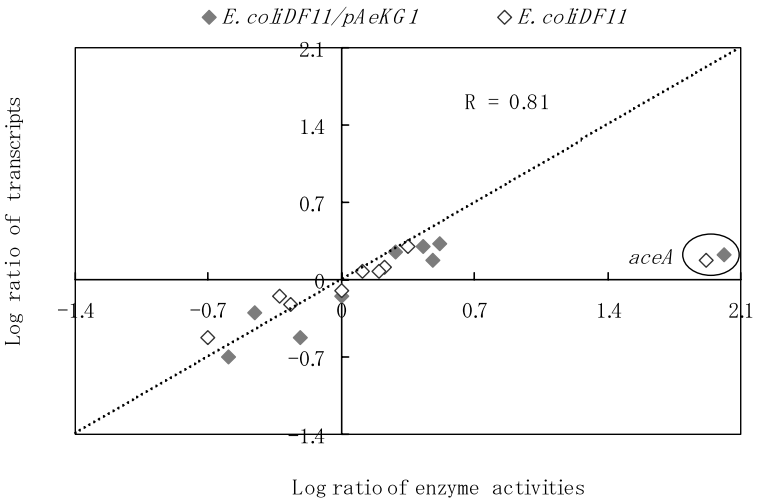

Fig. 7. The correlation between enzyme activities and mRNA transcripts on a log–log scale.

using [U–$^{13}C_6$] glucose-labeling experiments and metabolic flux ratio analysis provide evidence for the PP pathway as the primary route of glucose catabolism in *pgi* mutant *E. coli* (Canonaco et al., 2001). However, the measurement of ED pathway enzyme showed almost negligible activity (data not shown).

Basically, reoxidation of NADPH can potentially be achieved by three reactions in *E. coli*: (i) the NADPH-dependent malic enzyme; (ii) the membrane-bound transhydrogenase *pnt*AB (Clarke et al., 1986); and (iii) the soluble transhydrogenase *udh*A (Boonstra et al., 1999). Significant involvement of the malic enzyme in NADPH reoxidation can be excluded, since virtually no pyruvate originates from malate (Canonaco et al., 2001), and this result was consistent with our measurement of no malic enzyme activity. However, expression of *mae*B (coding for malic enzyme) was moderately downregulated in both *pgi*

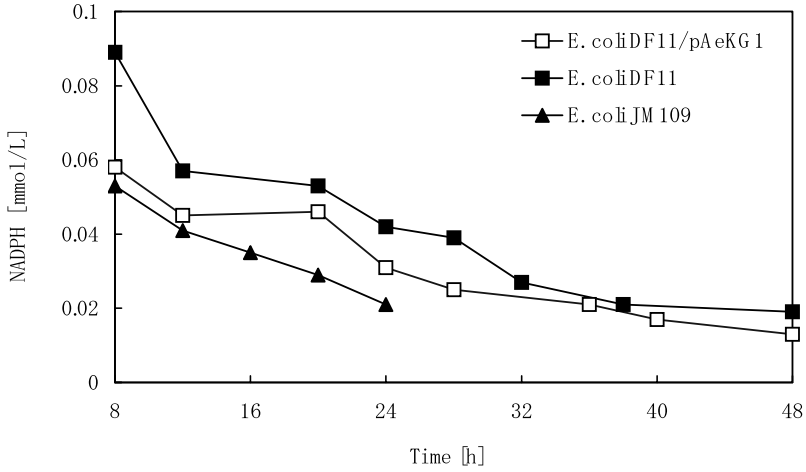

Fig. 8. The measurements of intracellular NADPH concentration of control *E. coli* JM109, *pgi* mutant *E. coli* DF11 and recombinant *pgi* mutant *E. coli* DF11/pAeKG1.

mutants *E. coli* compared to that in *E. coli* JM109 (Figs. 4 and 5) indicating that a different kind of regulation for *mae*B after transcription initiation. Similarly, *pnt*AB is unlikely to catalyze sufficient reoxidation of NADPH since *pgi pnt*AB double mutant grows as slowly as the *pgi* mutant (Hanson and Rose, 1980), which means that additional knockout of *pnt*AB does not further reduce the rate of glucose catabolism. The primary metabolic function of *pnt*AB appears to be in the generation of NADPH, since *zwf pnt* double mutant grows slower than the *zwf* mutant (Hanson and Rose, 1980), as is expected when *pnt*AB produces NADPH in the absence of PP pathway flux (in the *zwf* mutant). Expression levels of *pnt*A and *pnt*B were upregulated in both *pgi* mutants compared to those in control strain (see Figs. 4 and 5), indicating that inactivation of phosphoglucose isomerase leads to the overproduction of NADPH in PP pathway, which apparently disturbs the reducing power balance in *pgi* mutant and that ultimately reduces the biomass synthesis as was shown in Fig. 1b. Overexpression of soluble transhydrogenase *udh*A in *pgi* mutant *E. coli* increased specific growth rate by about 25% that evidenced the ability of the soluble transhydrogenase *udh*A in the reoxidation of NADPH (Canonaco et al., 2001). In this study, downregulation of *udh*A gene expression in both *pgi* mutants indicates an insufficient reoxidation of NADPH. It was observed from our experimental results that the expression of *phb* genes in *pgi* knockout *E. coli* increased the biomass production (Fig. 1c) as compared with the *pgi* mutant without *phb* genes (Fig. 1b). Obviously, PHB accumulation within cells increases the overall biomass concentration even though the growth rate becomes low. Therefore, the calculation of true cell mass subtracting the PHB concentration from the total biomass is recommended to get the actual biomass comparing with the biomass of non-PHB producers. Expression of *phb* genes in *E. coli* DF11/pAeKG1 increased the true cell mass by about 19% and this phenomenon might be the evidence for a physiological role of the acetoacetyl-CoA reductase encoded by *phb*B gene in the reoxidation of NADPH. The measurement of NADPH concentration supports our experimental observations. The concentration of NADPH was much higher in *E. coli* DF11 than those of *E. coli* JM109 (see Fig. 8). However, the NADPH concentration became lower for *E. coli* DF11/pAeKG1 as compared with that of *E. coli* DF11, which clearly evidenced the vital involvement of *phb*B genes in NADPH reoxidation.

Since glucose is metabolized exclusively via pentose phosphate pathway in *pgi* mutant, the important glycolysis metabolite glyceraldehyde-3-P is directly supplied from PP pathway. Glyceraldehyde-3-P is one of the important precursor metabolites for the synthesis of isopentenyl diphosphate (IPP) that acts as a carrier in the synthesis of a number of cell envelopes and extracellular polymers (e.g. peptidoglycan, lipopolysaccharide, techoic acids, etc.). As a result, large fraction of glyceraldehyde-3-P is being consumed to maintain the glycolytic flux for biomass production and to provide the precursor metabolites for PHB synthesis. Therefore, the expression of the gene *gap*A (12.4-fold increase) in *E. coli* DF11/pAeKG1 might have been upregulated highly to enhance the rate of conversion from glyceraldehyde-3-P (first three carbon metabolite of glycolysis) to glycerate-1,3-diphosphate to provide increasing demand for acetyl-CoA, since the PHB synthesis pathway competes for acetyl-CoA with three other metabolic pathways (Lee and Chang, 1995; Lee et al., 1994).

The possible reason of *pps*A upregulation in *E. coli* DF11/pAeKG1 might be due to the shortage of PEP and GAP. Another gene *pck*A also upregulated in *E. coli* DF11/pAeKG1, which also implies the above idea. It may be noted that *pps*A upregulation might also be due to the effect of global regulatory gene, *fru*R since *pps*A was found to be positively regulated by *fru*R (Saier and Ramseier, 1996). The *ppc* gene (coding for phosphoenol pyruvate carboxylase) was downregulated in both *E. coli* DF11 and *E. coli* DF11/pAeKG1, whereas *pck*A gene was upregulated in both strains. The regulation of these genes has not been fully elucidated, although it has been shown that *ppc* overexpression affects acetate production (Farmer and Liao, 1997). Thus, the downregulation of *ppc* expression that occurs during PHB synthesis may result in an increase in the acetate

production flux (Table 2). Furthermore, during growth in glucose, *ppc* is the major route to the aspartate family of amino acids. Therefore, down-regulation of *ppc* has to be compensated by another anaplerotic pathway.

The pyruvate dehydrogenase (*pdh*) complex is composed of multiple copies of three separate enzymes: pyruvate dehydrogenase (encoded by *ace*E), dihydrolipoate transacetylase (encoded by *ace*F) and lipoamide dehydrogenase (encoded by *lpd*A). The reactions of the *pdh* complex serve to interconnect the metabolic pathways of glycolysis and fatty acid synthesis to the TCA cycle as well as to the PHB synthetic route. Although the activity of the *pdh* complex is highly regulated by a variety of allosteric effectors and by covalent modification, it can be expected that a reduced level of expression of these genes, i.e. reduced level of synthesis of this complex would limit the accumulation of acetyl-CoA and thus PHB synthesis.

The significant upregulation of the gene *fkp*A in *E. coli* DF11/pAeKG1 may be considered to be due to the fact that *fkp*A plays an active role either as folding catalysts or as chaperones in extracytoplasmic compartments (Missiakas et al., 1996). Furthermore, the takeover of the cytosolic space by PHB granules may disturb the normal intracellular architecture such as chromosomal attachment and may consequently result in the heat shock response. Bacteria naturally accumulating PHB synthesize phasin protein that covers the surface of PHB granules. *E. coli* does not produce PHB naturally, and therefore does not have the phasin gene (Wieczorek et al., 1995). Therefore, the hydrophobic PHB granules are in direct contact with intracellular biomolecules including DNA, RNA, and proteins. Certainly, this will become a major stress on the cells for several possible reasons including protein denaturation on the surface of PHB granules. This unfavorable condition generated by PHB accumulation might have resulted in the highest expression of *rps*A (coding 30S ribosomal protein S1) in *E. coli* DF11/pAeKG1 (see Fig. 5), and it may have caused further increase in the soluble protein concentration (see Table 2) since S1 is the largest ribosomal protein (Wittmann, 1974) present in the small subunit of the *E. coli* 70S ribosome that has a pivotal role in stabilizing the mRNA on the ribosome for protein synthesis (Sengupta et al., 2001). Moreover, protein S1 has been reported to be necessary in some cases for translation initiation (Tzareva et al., 1994) and for translation elongation (Potapov and Subramanian, 1992). However, expression of the gene *rps*A could be the effect of acetate accumulation as was observed by Arnold et al. (2001). In our study, highest expression of the gene *rps*A in *E. coli* DF11/pAeKG1 was not due to the effect of acetate accumulation, since if it was caused by acetate effect, its expression should be decreased. Therefore, the highest amount of soluble protein synthesis in *pgi* mutant having *phb* genes was due to the effect of PHB accumulation that ultimately resulted in the highest expression of the gene *rps*A. This phenomenon implies that protein synthesis capacity in *E. coli* DF11/pAeKG1 was much increased in the presence of plasmid as evidenced in Table 2.

Acknowledgements

It is acknowledged that the research was supported in part by a grant from New Energy and Industrial Technology Development Organization (NEDO) of the Ministry of Economy, Trade and Industry of Japan (Development of Technological Infrastructure for Industrial Bioprocess Project).

Appendix A

G6P	Glucose-6-phosphate
F6P	Fructose-6-phosphate
$F1,6P_2$	Fructose-1,6-diphosphate
G3P	Glyceraldehyde-3-phosphate
PEP	Phosphoenol pyruvate
PYR	Pyruvate
AcCoA	Acetyl-coenzymeA
ICT	Isocitrate
SUC	Succinate
MAL	Malate
OAA	Oxaloacetate

6PGnt	6-Phosphogluconate
Ru5P	Ribulose-5-phosphate
R5P	Ribose-5-phosphate
X5P	Xylulose-5-phosphate
S7P	Sedoheptulose-7-phosphate
E4P	Erythrose-4-phosphate
AcAcCoA	Acetoacetyl-coenzymeA
HBCoA	Hydroxybutyryl-coenzymeA

References

Akiyama, H., Kanai, S., Hirano, M., Kumei, Y., Shimokawa, H., Katano, H., Hara, E., Song, S., Mukai, C., Nagaoka, S., 1996. An improved quantitative RT-PCR fluorescent method for analysis of gene transcripts in the STS-65 space shuttle experiment. J. Biotechnol. 47, 325–333.

Arcelana-Panlilio, M.Y., Schultz, G.A., 1993. Analysis of messenger RNA. Meth. Enzymol. 225, 303–328.

Arfin, S.T., Long, A., Ito, E.T., Tolerri, L., Riehle, M.M., Paegle, E.S., Hatfield, G.W., 2000. Global gene expression profiling in *Escherichia coli* K12: the effects of integration host factor. J. Biol. Chem. 275, 29672–29684.

Arnold, C.N., Mcelhanon, J., Lee, A., Leonhart, R., Siegele, D.A., 2001. Global analysis of *Escherichia coli* gene expression during the acetate-induced acid tolerance response. J. Bacteriol. 183, 2178–2186.

Arora, K.K., Pedersen, P.L., 1995. Glucokinase of *Escherichia coli*: induction in response to the stress of overexpressing foreign proteins. Arch. Biochem. Biophys. 319, 574–578.

Bergmeyer, H.U., 1989. Methods of Enzymatic Analysis, vol. VII, Third Edition. VCH Publishers, Weinheim, Germany, pp. 261–267.

Boonstra, B., French, C.E., Wainwright, I., Bruce, N.C., 1999. The *udh*A gene of *Escherichia coli* encodes a soluble pyridine nucleotide transhydrogenase. J. Bacteriol. 181, 1030–1034.

Braunegg, G., Sonnteither, B., Lafferty, R.M., 1978. A rapid gas chromatography method for the deteremination of poly-β-hydroxybutyric acid in microbial biomass. Eur. J. Appl. Microbiol. Biotechnol. 6, 29–37.

Brown, T.D., Jones-Mortimer, M.C., Kornberg, H.L., 1977. The enzymic interconversion of acetate and acetyl-coenzyme A in *Escherichia coli*. J. Gen. Microbiol. 102, 327–336.

Brucato, S., Harduin-Lepers, A., Godard, F., Bocquet, J., Villers, C., 2000. Expression of glypican-1, syndecan-1 and syndecan-4 mRNAs protein kinase C-regulated in rat immature Sertoli cells by semi-quantitative RT-PCR analysis. Biochem. Biophys. Acta 1474, 31–40.

Canonaco, F., Hess, T.A., Heri, S., Wang, T., Szyperski, T., Sauer, U., 2001. Metabolic flux response to phosphoglucose isomerase knock-out in *Escherichia coli* and impact of overexpression of the soluble transhydrogenase UdhA. FEMS Microbiol. Lett. 204, 247–252.

Clarke, D.M., Loo, T.W., Gillam, S., Bragg, P.D., 1986. Nucleotide sequence of the *pnt*A and *pnt*B genes encoding the pyridine nucleotide transhydrogenase of *Escherichia coli*. Eur. J. Biochem. 158, 647–653.

DeRisi, J.L., Iyer, V.R., Brown, P.O., 1997. Exploring the metabolic and genetic control of gene expression on a genomic scale. Science 278, 680–686.

Dieffenbach, C.W., Dveksler, G.S., 1995. PCR Primer: A Laboratory Manual. Cold Spring Harbor Laboratory Press, Cold Spring Harbor, NY.

Farmer, W.R., Liao, J.C., 1997. Reduction of aerobic acetate production by *Escherichia coli*. Appl. Environ. Microbiol. 63, 3205–3210.

Ferea, T.L., Botstein, D., Brown, P.O., Rosenzweig, R.F., 1999. Systematic changes in gene expression patterns following adaptive evolution in yeast. Proc. Natl. Acad. Sci. USA 96, 9721–9726.

Foley, K.P., Leonard, M.W., Engel, J.D., 1993. Trends Genet. 9, 380.

Grunberg-Manago, M., 1996. Regulation of the expression of aminoacyl-tRNA synthetases and translation factors. In: Neidhardt, F.C., Curtiss, R., III, Ingraham, J.L., Lin, E.C.C., Low, K.B., Magasanik, B., Reznikoff, W.S., Riley, M., Schaechter, M., Umbarger, H.E. (Eds.), *Escherichia coli* and *Salmonella*: Cellular and Molecular Biology, 2nd ed. ASM Press, Washington, DC, pp. 1432–1457.

Hanson, R.L., Rose, C., 1980. Effects of insertion mutation in a locus affecting pyridine nucleotide transhydrogenase (*pnt*::*Tn5*) on the growth of *Escherichia coli*. J. Bacteriol. 141, 401–404.

Harrison, D.C., Medhurst, A.D., Bond, B.C., Campbell, C.A., Davis, R.P., Philpott, K.L., 2000. The use of quantitative RT-PCR to measure mRNA expression in a rat model of focal ischemia-caspases as a case study. Mol. Brain Res. 75, 143–149.

Iyer, V.R., Eisen, M.B., Ross, D.T., Schuler, G., Moore, T., Lee, J.C.F., Trent, J.M., Staudt, L.M., Hudson, M.S., Boguski, D., Lashkari, D., Shalon, D., Botstein, D., Brown, P.O., 1999. The transcriptional program in the response of human fibroblasts to serum. Science 283, 83–87.

Kao, C.M., 1999. Functional genomic technologies: creating new paradigms for fundamental and applied biology. Biotechnol. Prog. 15, 304–311.

Kidwell, J., Valentin, H.E., Dennis, D., 1995. Regulated expression of the *Alcaligenes eutrophus pha* biosynthesis gene in *Escherichia coli*. Appl. Environ. Microbiol. 61, 1391–1398.

Kwon, D.H., Osato, M.S., Graham, D.Y., El-Zaatari, F.A.K., 2000. Quantitative RT-PCR analysis of multiple genes encoding putative metronidazole nitroreductases from *Helicobacter pylori*. Int. J. Antimicrob. Agents 15, 31–36.

Lamed, R., Zeikus, J.G., 1980. Glucose fermentation pathway of *Thermonaerobium brockii*. J. Bacteriol. 141, 1251–1257.

Lee, S.Y., Chang, H.N., 1995. Production of poly(3-hydroxybutyric acid) by recombinant *Escherichia coli* strains:

genetic and fermentation studies. Can. J. Microbiol. 41, 207–215.

Lee, S.Y., Lee, K.M., Chang, H.N., Steinbüchel, A., 1994. Comparison of recombinant *Escherichia coli* strains for synthesis and accumulation of poly(3-hydroxybutyric acid) and morphological changes. Biotechnol. Bioeng. 44, 1337–1347.

Lowery, O.H., Rosbrough, J.N., Farr, A.L., Randall, R.J., 1951. Protein measurement with the folin-phenol regent. J. Biol. Chem. 193, 265–275.

Martin, B.R., 1987. The regulation of enzyme activity. In: Martin, B.R. (Ed.), Metabolic Regulation: A Molecular Approach. Oxford, London, Edinburgh, Boston, Palo Alto, Melbourne, pp. 12–27.

Missiakas, D., Betton, J.-M., Raina, S., 1996. New components of protein folding in extracytoplasmic compartments of *Escherichia coli* SurA, FkpA and Skp/OmpH. Mol. Microbiol. 21, 871–884.

Mocharla, H., Mocharla, R., Hodes, M.E., 1990. Gene 93, 271.

Park, S.-J., Gunsalus, R.P., 1995. Oxygen, iron, carbon, and superoxide control of fumerase *fum*A and *fum*C genes of *Escherichia coli*: role of the *arc*A, *fnr*, and *sox*R gene products. J. Bacteriol. 177, 6255–6262.

Park, S.-J., McCabe, J., Turna, J., Gunsalus, R.P., 1994. Regulation of citrate synthase (*glt*A) gene of *Escherichia coli* in response to anaerobiosis and carbon supply: role of the *arc*A gene product. J. Bacteriol. 176, 5086–5092.

Park, S.-J., Tseng, C.-P., Gunsalus, R.P., 1995a. Regulation of succinate dehydrogenase (*sdh*CDAB) operon expression in *Escherichia coli* in response to carbon supply and anaerobiosis: role of *Arc*A and *Fnr*. J. Bacteriol. 15, 473–482.

Park, S.-J., Cotter, P.A., Gunsalus, R.P., 1995b. Regulation of malate dehydrogenase (*mdh*) gene expression in *Escherichia coli* in response to oxygen, carbon, and heme availability. J. Bacteriol. 177, 6652–6656.

Park, S.-J., Chao, G., Gunsalus, R.P., 1997. Aerobic regulation of the *suc*ABCD genes of *Escherichia coli*, which encode α-ketoglutarate dehydrogenase and succinyl coenzyme A synthetase: role of *Arc*A, *Fnr*, and the upstream *sdh*CDAB promoter. J. Bacteriol. 179, 4138–4142.

Parvin, R., 1969. Citrate synthase from rat liver. In: Lowenstein, J.M. (Ed.), Methods in Enzymology. Academic Press, New York, Tokyo, pp. 16–19.

Pearse, A.J., Wolf, R.E., 1994. Determination of the growth rate-regulated steps in expression of *Escherichia coli* K-12 *gnd* gene. J. Bacteriol. 176, 115–122.

Potapov, A.P., Subramanian, A.R., 1992. Biochem. Int. 27, 745–753.

Richmond, C.S., Glasner, J.D., Mau, R., Jin, H., Blattner, F.R., 1999. Genome wide expression profiling in *Escherichia coli* K-12. Nucl. Acids Res. 27, 3821–3835.

Saier, M.H., Jr., Ramseier, T.M., 1996. The catabolite repressor/activator (Cra) protein of enteric bacteria. J. Bacteriol. 178, 3411–3417.

Salas, M., Vinuela, E., Sols, A., 1965. Spontaneous and enzymatically catalyzed anomerization of glucose-6-phosphate and anomeric specificity of related enzymes. J. Biol. Chem. 240, 561–568.

Sambrook, J., Russell, D.W., 2001. Molecular Cloning: A Laboratory Manual, 3rd ed. Cold Spring Harbor Laboratory Press, Cold Spring Harbor, NY.

Samuelov, N.S., Lamed, R., Lowe, S., Zeikus, J.G., 1991. Influence of CO_2-HCO_3^- levels and pH on growth, succinate production, and enzyme activities of *Anaerobiospirillum succiniciproducens*. Appl. Environ. Microbiol. 57, 3013–3019.

Sengupta, J., Agrawal, R.K., Frank, J., 2001. Visualization of protein S1 within the 30S ribosomal subunit and its interaction with messenger RNA. Proc. Natl. Acad. Sci. USA 98, 11991–11996.

Siebert, P.D., Larrick, J.W., 1991. Nature 359, 557.

Singer-Sam, J., Riggs, A.D., 1993. Quantitative analysis of messenger RNA levels: reverse transcription polymerase chain reaction single nucleotide primer extension assay. Meth. Enzymol. 225, 344–351.

Shi, H., Nikawa, J., Shimizu, K., 1999. Effect of modifying metabolic network on poly-3-hydroxybutyrate biosynthesis in recombinant *Escherichia coli*. J. Biosci. Bioeng. 87, 666–677.

Sridhar, J., Eiteman, M., Wiegel, J.W., 2000. Elucidation of enzymes in fermentation pathways used by *Clostridium thermosuccino* genes growing on inulin. J. Environ. Microbiol. 66, 246–251.

Tao, H., Bausch, C., Richmond, C., Blattner, F.R., Conway, T., 1999. Functional genomics: expression analysis of *Escherichia coli* growing on minimal and rich media. J. Bacteriol. 181, 6425–6440.

Tzareva, N.V., Makhno, V.I., Boni, I.V., 1994. FEBS Lett. 337, 189–194.

Van der Werf, M.J., Guettle, M.V., Jain, M.K., Zeikus, J.G., 1997. Environmental and physiological factors affecting the succinate product ratio during carbohydrate fermentation by *Actinobacillus* sp. 130Z. Arch. Microbiol. 167, 332–342.

Wieczorek, R.A., Pries, A., Steinbüchel, A., Mayer, F., 1995. Analysis of a 24-kilodalton protein associated with the polyhydroxyalkanoic acid granules in *Alcaligens eutrophus*. J. Bacteriol. 177, 2425–2435.

Wilson, M., DeRisi, J., Kristensen, H.H., Imboden, P., Rane, S., Brown, P.O., Schoolnik, G.K., 1999. Exploring drug-induced alterations in gene expression in *Mycobacterium tuberculosis* by microarray hybridization. Proc. Natl. Acad. Sci. USA 96, 12833–12838.

Wittmann, H.G., 1974. In: Namura, M., Tissieres, A., Lengyel, P. (Eds.), Robosomes. Cold Spring Harbor Laboratory Press, Plainview, NY, pp. 93–114.